Monitoring Shortwave Fadeout (SWF) Across North America using SuperDARN HF Radar Observations

S. Chakraborty[1], J.M. Ruohoniemi[1], and J.B.H. Baker[1]

[1]**Virginia Tech, Blacksburg, VA, 24061, http://www.vt.edu/ Virginia, USA**

ABSTRACT

Shortwave fadeout (SWF) is a well-known radio wave anomaly which occurs following solar flares and leads to severe disruption of trans-ionospheric HF systems. The disruption is produced by flare-enhanced soft and hard X-rays which penetrate to the D-layer where they dramatically enhance ionization leading to heavy HF absorption over much of the dayside for an hour or more. In this paper, we describe how Super Dual Auroral Radar Network (SuperDARN) observations can be exploited to monitor SWF events in real-time. Specifically, the number of SuperDARN ground-scatter echoes drops suddenly (≈ 1 min) after a solar flare, reaching a maximum depth of suppression within a few tens of minutes, and then recovering to pre-SWF conditions over half an hour or so. The depth of echo suppression depends on the intensity of the flare, zenith angle, and radio wave frequency. Furthermore, ground-scatter echoes typically exhibit a sudden phase change leading to a dramatic increase in apparent Doppler velocity (or so-called "velocity flash") which precedes the dropout in ground-scatter echoes. We report here on the characterization of these SWF effects in SuperDARN ground-scatter observations produced by several M and X-class solar flares. We also describe several Python-based tools that have been developed for real-time detection of SWF in SuperDARN observations across North America and thus serve as an effective space weather capability for prompt detection of impending disruption to HF communications.

Keywords: Shortwave Fadeout, Monitoring Tool, SWF, SuperDARN, Space Weather, HF Communication

INTRODUCTION

A solar flare event is one of the most extreme processes occurring on the Sun. It is the sudden flash of increase in brightness observed near the Sun's surface which involves a very broad spectrum of emissions. During a solar flare, the Sun emits extreme ultraviolet (EUV) and X-rays, in general, enormous energy spikes to the outer space with variable duration, ranging from few minutes to few hours which increase the ionization in ionosphere. This sudden increase of plasma density produces a sudden increase in radio-wave absorption that is most severe in the high frequency (HF) ranges, commonly known as Shortwave Fadeout (SWF). Shortwave fadeout is directly related to EUV and X-rays emitted by the Sun, which propagates at the speed of light which takes few minutes (≈ 8 m) to reach Earth's atmosphere. That makes it the first space weather effect following a solar activity. Incoming solar flux hits the day side of the Earth, which makes SWF a daytime phenomenon.

Modern civilization is dependent on sophisticated electronics devices, whose operations are vastly dependent on radio wave communication channel. SWF is more affected near HF band of spectrum, thus, any HF communication or wireless instrument (such as armature or HAM radio, OTH Radar, Flight Communication [Jason J. Neal (2013)]) that uses ionosphere-earth spherical cavity resonator to transfer information from one ground station to other is going to experience a transmission loss. This motivates a tool to monitor SWF in real-time that can provide the event impact time and location, the intensity of HF radio wave absorption at different frequencies and its spread across the globe.

In recent years due to technological advancements, we have satellites having a sophisticated device on board, which can read solar flux intensity, commonly known as solar X-ray imager. That can also be used to monitor the variation in the intensity of solar flare during the event and the effect of such variability on the shortwave fadeout. NOAA has a tool D-Region Absorption Prediction[NOAA (2015)][R. A. Akmaev and Nerne (2010)] commonly known as D-RAP2, which provides a absorption prediction at D-region due to solar flare and energetic particle precipitation. It process GOES X-ray imager data and provides real-time information related to SWF. It uses different empirical models to predict the intensity of SWF at different HF frequencies and also estimates the recovery times of the event. This DRAP2 model also monitors polar cap absorption phenomenon, which is radio wave absorption due to energetic particle precipitation at the polar cap regions [Sauer and Wilkinson (2008)][Jason J. Neal (2013)].

SuperDARN HF radar observations of daytime ground-scatter are strongly affected by SWF. A sudden onset of absorption is commonly registered over 1 – 2 minutes leading to almost complete suppression of echoes over a few 10s of minutes and recovery to pre-SWF conditions over half an hour. We can exploit SuperDARN observations of ground scatter to monitor SWF in real-time. In this presentation we describe a Python-based tool that can monitor the ground-scatter observations and detects SWF across North America retrospectively, using the network of SuperDARN radars. We also discuss the pattern recognition technique for SWF in the radar observations and the development of an effective space weather capability for detecting this source of disruption to HF communication channels.

OVERVIEW OF SWF SEEN IN SUPERDARN GROUND-SCATTER

The Super Dual Auroral Radar Network (SuperDARN) is an international scientific radar network consisting a chain of high frequency (HF) radars located in both the Northern and Southern Hemispheres. SuperDARN radars are primarily used to map high-latitude plasma convection in the F region of the ionosphere, but the radars are also used to study a wider range of geophysical phenomenon.

Terrestrial Surface Scatter or Ground-Scatter

Working principle of SuperDARN is based on radio wave refraction due to the ionosphere and $\vec{E} \times \vec{B}$ drift of the plasma. Most of the SuperDARN radar operates within 8 MHz to 18 MHz frequency band, that makes the transmitted radio waves of SuperDARN more sensitive to ionospheric refraction. SuperDARN nighttime observations are populated with ionospheric scatters i.e. half-hop or one-and-half-hop scatters. But during the day ionosphere is denser than night, that enforces radio waves to bend more towards ground and rays are unable to reach the height to meet $\vec{E} \times \vec{B}$ orthogonality condition. These radio waves (directed towards the ground) reach the ground and reflected back to radar through the same path. The backscatter returns from the terrestrial surface transit the ionosphere four times as illustrated in the figure (1) and simulate the operation of an HF communications link. In the figure rays at different elevation angles are projected towards ionosphere. All the rays bend towards ground due to a high population density of the plasma.

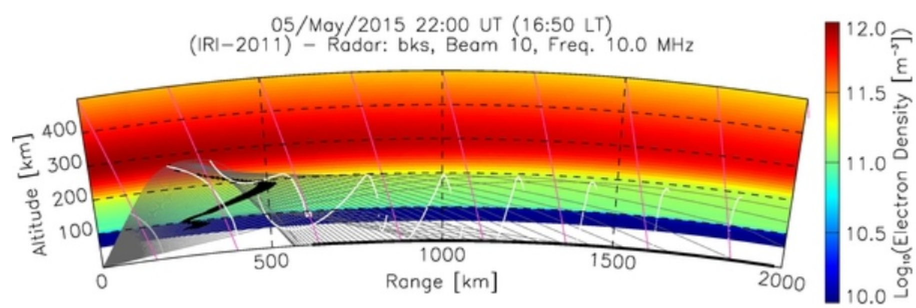

Figure 1. Ray-tracing of a SuperDARN radar (near Blackstone, operating at 10 MHz) on a typical day. Rays bend towards ground due to low refractive index or high accumulation of plasma in the lower ionosphere. Rays get reflected from the terrestrial land surface and follow the same path to get back to the radar receiver. It's a proper demonstration of an HF two-way communication channel. Blue colored region (below 100 km) is the D-region of the ionosphere.

SuperDARN Ground-Scatter Observation

SuperDARN daytime observations are populated by the ground-scatter. Doppler velocity and spectral width of SuperDARN ground-scatters echoes are very small than that of ionospheric echoes. Doppler velocity of ground-scatter is less than $\pm 10\ m/s$, whereas ionospheric scatter has a Doppler velocity in the range of $\pm 100 - 200\ m/s$. Figure (2) presents SuperDARN velocity field-of-view (FoV) plot of a

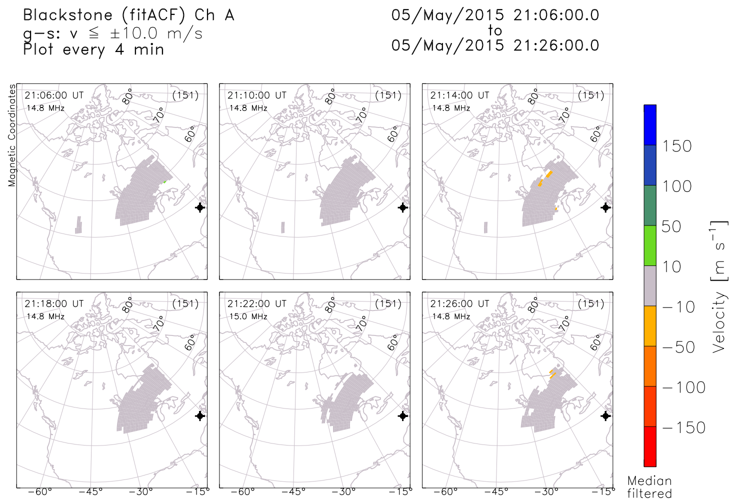

Figure 2. Field-of-view (FoV) plot of a SuperDARN radar (near Blackstone, operating at 14.8 MHz) on a typical day. Each panel is a snapshot of radar scan taken at different time. This FoV plot is showing a line of sight Doppler velocity of ground scatter (in gray). Most of the backscatter has velocity less than $\pm 10\ m/s$.

typical day. The figure also provide evidence about two facts, first SupderDARN day time observation is populated with ground-scatter and the second is most of the ground-scatter has low velocity.

SuperDARN Ground-Scatter Observation During an SWF Event

Figure (3) presents the FoV plot during an SWF event on 5^{th} May, 2015 around 22.10 hours. Figure (3) depicts some observational difference between regular day and an SWF event. During an SWF SuperDARN ground-scatter observation shows following patterns which are very different from a regular day observation.

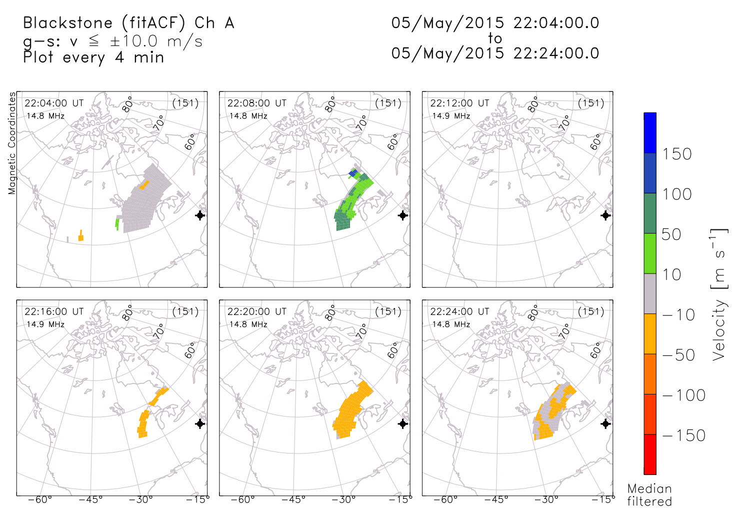

Figure 3. Field-of-view (FoV) plot of a SuperDARN radar (near Blackstone, operating at 14.8 MHz) during an SWF event on 5^{th} May, 2015 at $22:10$ hours. Each panel is a snapshot of radar scan taken at different time during the event.

a. Ground-scatter echoes wipe out completely (Number of echoes $= 0$) in 1^{st} row 3^{rd} panel.

b. Just before ground-scatter wipes out 1^{st} row 2^{nd} panel shows a sudden enhancement in ground-scatter velocity which is comparable to mid-latitude ionospheric scatter.

c. During recovery ground-scatter velocity goes slightly negative as shown in 2^{nd} row.

CHARACTERISTICS OF A TYPICAL SWF SIGNATURE

This section presents a detailed analysis of different characteristics of SuperDARN observation during an SWF event. Daytime SuperDARN ground-scatters are heavily impacted by SWF events. Figure (4) presents a plot shows variability in a number of average ground-scatter echoes during SWF event on 5^{th} May 2015, around $22:10$ UT. In that figure (4) top panel presents operating frequency of the radar, 2^{nd}

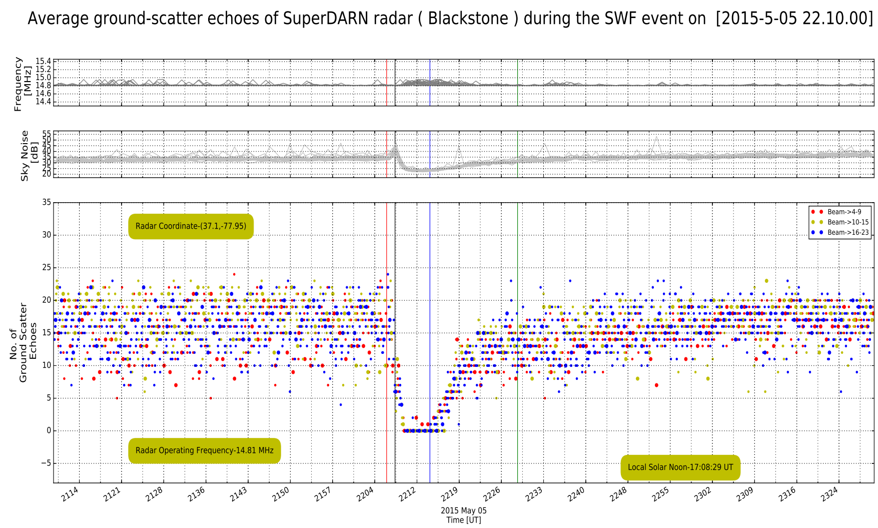

Figure 4. Different phases of ground-scatter echoes observation in SuperDARN radar(Blackstone) on 5^{th} May, 2015, around $22:10$ UT. Red dots represents a number of average ground-scatters of beam $4-9$ (due west looking beam), yellow dots represents the number of average ground-scatters of beam $10-15$(due north looking beam), and blue dots represents the number of average ground-scatters of beam $16-23$ (due east looking beam). Vertical lines are the demarcation between phases. Red line is centered at $22:06:49$UT$\pm 10.7s$, black line is centered at $22:08:15$ UT$\pm 6.9s$, blue line is centered at $22:14:12$UT$\pm 6.9s$, green line is centered at $22:29:09$UT$\pm 7s$.

panel shows incoming galactic noise, and the bottom panel shows a number of average ground-scatter echoes for each beam. The geographic location of the radar is $(37.8^o, -77.5^o)$, and during this SWF event, geographic location of the sub-solar point is $(23.6^o, -150.5^o)$. So, during this event Blackstone radar has a solar zenith angle of $\approx 69^o$.

Different phases are shown in the figure (4), and the vertical lines are the demarcation between the consecutive phases. These demarcation lines are determined by an algorithm. These different phases are listed below –

i. Pre-SWF or stable ground-scatter [Before red line and after green line]: As the name suggests pre-SWF or stable ground-scatter phase is the stable phase when no radio wave anomaly is detected by the ground-scatter.

ii. Onset of the event [After red line and before black line]: This is one of the precursor phases of the SWF event. During this phase, we can see a significant deviation in a number of ground-scatter echoes from the previous stable mean value. Duration of this phase mainly depends on the class of the flare. Variability of the phase timing is loosely dependent on solar zenith angle and radar operating a frequency of the radar.

iii. Blackout of the event [After black line and before blue line]: This is the main phase of the SWF event. During this phase, HF radio wave undergoes heavy absorption. From the figure, we can estimate that most of the beams reached experienced heavy absorption and number of ground-scatter is almost zero. Variability of the phase timing is dependent on solar flare class, solar zenith angle and radar operating a frequency of the radar.

iv. Recovery of the event [After blue line and before green line]: This is the recovery phase of the SWF event. During this phase, ground-scatter recovers gradually from the absorption. Recovery takes the longest time among the different phases. Unlike onset, recovery of the SWF event is much more gradual. Variability of the phase timing is dependent on solar flare class, solar zenith angle and radar operating a frequency of the radar.

Velocity Flash of Ground-Scatter Echoes

Daytime ground-scatter observation of SuperDARN radars often undergoes a velocity flash during an SWF event. Just like onset phase of the SWF in ground-scatter observation, it's also a precursor to the event. Rapid change in ground-scatter phase resulted in this velocity flash. The phase shift is positive in nature, and the intensity of the phase shift is dependent solar flare class, solar zenith angle, and radar operating a frequency of the radar.

Figure (5) presents the timing offset of the ground-scatter velocity and power absorption. Top panel presents average ground-scatter velocity, and bottom panel presents average ground-scatter power. Vertical lines present the timing of the velocity flash start (Red) and velocity peak (black). Red line is centered at 22 : 07 : 33UT and the black line are centered at 22 : 08 : 00 UT. From the figure, it's pretty evident that before going to blackout phase ground-scatter experience a positive phase shift. Also note that at the early recovery phase ground-scatter is slightly negative, and gradually reaches to zero.

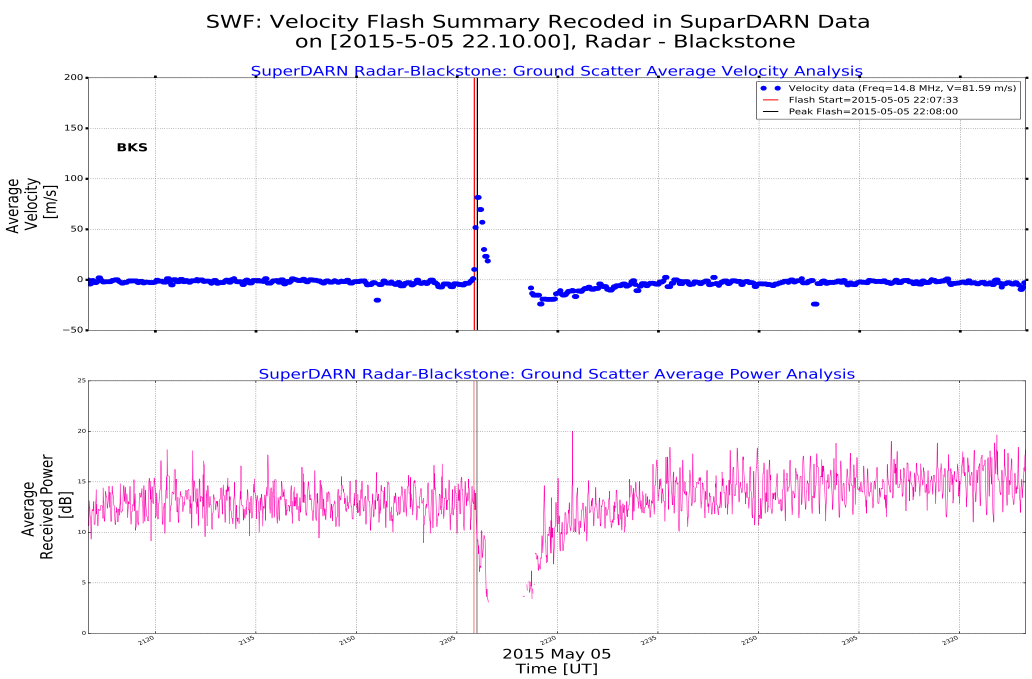

Figure 5. Sudden increase in average ground-scatter velocity in SuperDARN radar(Blackstone) on 5^{th} May, 2015, around 22 : 10 UT. The top panel shows average ground-scatter velocity, bottom panel shows average ground scatter power. Vertical lines present the timing of the velocity flash start (Red) and velocity peak (black). Red line is centered at 22 : 07 : 33UT and the black line are centered at 22 : 08 : 00 UT.

SPACE WEATHER MONITORING TOOL

This section presents a brief description of a Python-based SWF monitoring tool. This monitoring tool exploits the basic characteristics of SWF effect seen in daytime SuperDARN ground-scatter to provide a real-time space weather monitoring capability. This tool uses a subnetwork of SuperDARN radars spread across the North America. This tools uses the statistical data analysis techniques to identify the SWF patterns in mid and high latitude SuperDARN radars observations. It identifies the different phases of the SWF seen in the ground-scatter, and notifies by changing the color of the different devices (radars, satellites shown in different geometrical shapes) as shown in the figure (6). Tool fetches data

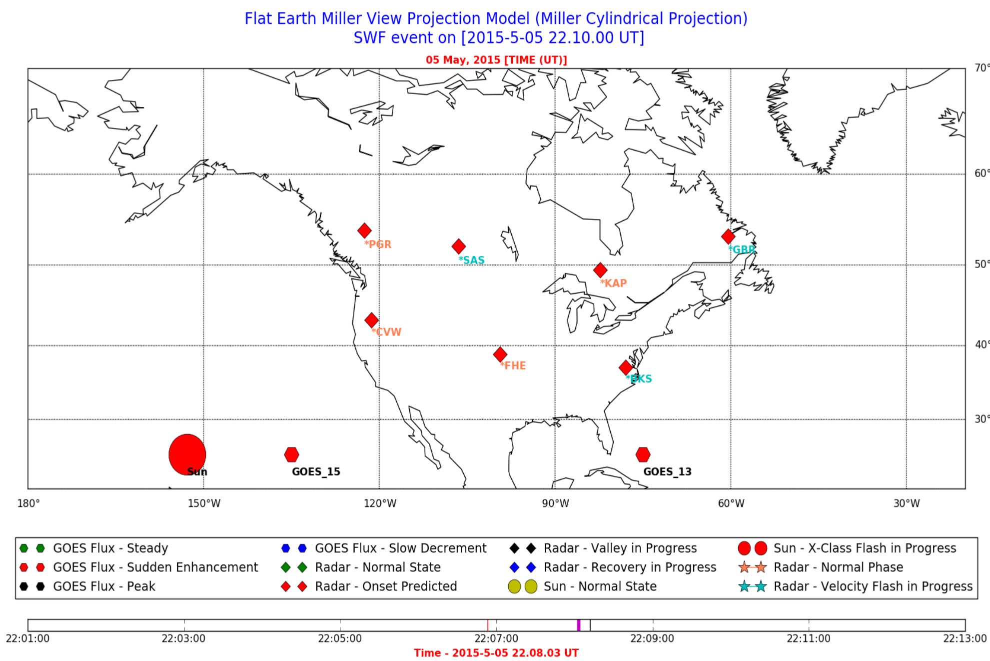

Figure 6. Python-based SWF monitoring tool. One snapshot of the time-lapse of the SWF event during 5^{th} May, 2015, around 22 : 10 UT. Big circle is Sun, two hexagons shows data variation of GOES X-ray imager data, and rhombus are the SuperDARN radars.

from GOES-15 and GOES-13 satellites to get the information of solar flares. Figure (6) shows a map of North America with different instruments (located at different places) by different geometrical shapes. Big circle is Sun, two hexagons shows data variation of GOES X-ray imager data, and rhombus are the SuperDARN radars. All of these geometrical shapes changes color according to the different phases of SWF. Different colors are associated with different phases of SWF and the color description is given at the bottom of the figure. This tool can be used to monitor the effect of SWF and spread across the globe.

Statistical Method to Detect Different Phases of SWF

This section presents the idea how Python-based tool detects any SWF pattern in the SuperDARN observation. Techniques are mostly statistical and hence simple to understand. SuperDARN ground-scatter echoes are impacted significantly during an SWF event and alters the typical daytime ground-scatter pattern. This tool exploits this knowledge to detect the pattern of an SWF event from the ground-scatter. Following algorithm gives an idea about the detection mechanism of the different phases of SWF event.

Data: SuperDARN Observations
Result: Background variation in SuperDARN ground-scatter
calculate background variation of SuperDARN ground-scatter;
1. Mean E;
2. Standard Deviation σ;
3. Running mean E_r with a specific window;
4. Running standard deviation σ_r with a specific window;
Save these information as a knowledge for future use;

Algorithm 1: Detection of steady background variation of ground-scatter observation.

Data: SuperDARN Observations with 10 minutes of history data.
Result: Timings of four different phases
#This method is called for each individual beam sounding;
Processes the data [Cleaning and noise reduction];
Get the background variation information in SuperDARN ground-scatter stored by Algo-1;
fit a line through the time-series data;
$slope \leftarrow \{\}$;$echoes\_count \leftarrow \{\}$;
for *All the data in this dataset* **do**
    $slope \leftarrow slope+$ calculate the slope of the line for one data point;
    $echoes\_count \leftarrow echoes\_count+$ calculate the number of echoes count for one data point;
end
Detect the SWF phases based on the *slope* and $echoes_count$ parameters;
Save this data as a history and wait for next call;

Algorithm 2: Detection of SWF pattern in SuperDARN observation.

DISCUSSION AND CONCLUSION

We performed statistical characterization of flares larger than X-1.0 from January 2013 to December 2015, and few flares larger than M-2.0 (12 in total). We are able to characterize SWF in terms of different physical parameters such as intensity of solar flare, solar zenith angle, the frequency of the transmitted radio wave. The intensity of SWF can be categorized under two different factors, firstly how much ground-scatter echoes are suppressed, and second is the duration of ground-scatter suppression. This tool uses statistical signal processing techniques to extract the timing information across different radars to get the SWF confirmation and provides the variability of SWF impact across the globe and it's evolution with time. Recent version of this monitoring tool doesn't use physical parameters information which control the intensity and duration of SWF. Embedding these information into the tool will provide more comprehensive capabilities for meticulous intensity and timing analysis.

REFERENCES

Jason J. Neal, Craig J. Rodger, J. C. G. (2013). Empirical determination of solar proton access to the atmosphere: Impact on polar flight paths. *Space Weather*, 11(S12002).

NOAA (2015). Global d-region absorption prediction documentation. http://www.swpc.noaa.gov/content/global-d-region-absorption-prediction-documentation.

R. A. Akmaev, A. Newman, M. C. C. S. and Nerne, E. (2010). Drap modelvalidation: I. scientific report. https://www.ngdc.noaa.gov/stp/drap/DRAP-V-Report1.pdf.

Sauer, H. H. and Wilkinson, D. C. (2008). Global mapping of ionospheric hf/vhf radio wave absorption due to solar energetic protons. *American Geophysical Union: Space Weather*, 6(S12002).